



Sputtering and reflection of self-bombardment of tungsten material



Guo-jian Niu^{a,b}, Xiao-chun Li^b, Qian Xu^b, Zhong-shi Yang^b, Guang-nan Luo^{a,b,c,d,*}

^a University of Science and Technology of China, Hefei, China

^b Institute of Plasma Physics Chinese Academy of Sciences, Hefei, China

^c Hefei Center for Physical Science and Technology, Hefei, China

^d Hefei Science Center of CAS, Hefei, China

ARTICLE INFO

Article history:

Received 7 December 2014

Received in revised form 23 January 2015

Accepted 23 January 2015

Keywords:

Cluster

Sputtering

Reflection

Molecular dynamics

Bombardment

ABSTRACT

In present research, the sputtering and reflection yield of self-bombardment of tungsten are investigated with the aid of molecular dynamics simulations. The source of sputtered and reflected atoms is detected by traced the original locations of sputtered and reflected atoms. Results show that for the reflected atoms no specific region exists which means cluster atoms are randomly reflected. But almost all of sputtered atoms are from a conical region under the landing point of cluster. So we can determine the sputtering yield by study the dimension of the sputtering region. Molecular dynamics shows the depth and radius of the conical are power functions of impacting energy. The effects of cluster size and temperature of target on sputtering and reflection rate are also preformed in present study. Both sputtering and reflection yield are proportion to cluster size in present cluster size, i.e. 66–2647 atoms. Higher target temperature can increase sputtering yield and deduce sputtering threshold energy, but little effect on reflection rate.

© 2015 Elsevier B.V. All rights reserved.

1. Introduction

Studies on the interactions between energetic cluster and solids can be applied in a series of fields such as cluster deposition [1,2], implantation [3,4], surface smoothing [5–7] and modifications [8–10], thin-film growth [11,12], secondary ion mass spectrometry (SIMS) [13,14], etc. The landing process of dust particles in planets and comets is also a further application of cluster impacting studies [15]. The cluster impacting process involves complicated physical process. For example, cluster can generate high-density and high-energy region under land point which is different from monatomic bombardment [12,4]. According to the impacting energy, clusters can soft land or implant on target, with different effects on target surface [3,16]. Soft landing clusters may form thin-film on the surface without damage it [17–19]. Implantation, however, can generate crater and produce sputtering atoms [20,21]. Sputtering yield of energetic clusters have been studied both experimentally and theoretically [22,23]. With the aid of molecular dynamics (MD) simulations, fruitful results have been obtained [24–27]. The angle dependence on sputtering has been discussed in Ref. [28] and other relative references. The effect of binding energy and mass in cluster-induced sputtering has been published

in Ref. [29]. Anders et al. used rational function to fit sputtering and reflection yield versus impacting energy [22,30].

In present research, we investigate the sputtering and reflection yield using molecular dynamics method. In particular, we want to learn about the relation between impacting energy and sputtering and reflection rate. The source of sputtered atoms is another question of our concern. The size of cluster and temperature of target are also taken into account in present study. Our results may be helpful to understand the mechanism of cluster sputtering.

2. Method

Molecular dynamics (MD) is applied to study the interaction between cluster and target. Both the materials of cluster and target are tungsten (W). An open code LAMMPS (Large-scale Atomic/Molecular Massively Parallel Simulator) code is used to perform MD simulation [31]. The model used to describe the interactions between W atoms is embedded atom method (EAM), namely, Finnis–Sinclair potential [32]. A repulsive pair potential named Ziegler–Biersack–Littmark (ZBL) is used when distance of two atoms is smaller than 1.6 Å to improve the compressibility at high pressures [33]. The structures of W clusters and W material are body-center-cubic (BCC) and the lattice constant for tungsten is 3.1652 Å. The (001) plane is normal to cluster impacting direction. Automatically adapted time step is used, the minimum and

* Corresponding author at: Institute of Plasma Physics Chinese Academy of Sciences, Hefei, China.

E-mail address: glnuo@ipp.ac.cn (G.-n. Luo).

maximum time step are 0.0001 fs and 1 fs, respectively. The system sizes are selected based on both energy and size of cluster and the maximum size of target is 2,894,400 atoms. For each collision case two different sizes are selected to exclude size dependence. Periodic boundary condition is for the directions perpendicular to the normal direction of W material surface and non-periodic boundary condition for the parallel direction. Three temperature of the system are selected, viz. 0 K, 300 K and 650 K. The shape of tungsten clusters is spherical and broken sphere in order to exclude shape dependence. The size of clusters ranges from 66 to 2647 atoms/cluster and the energy is 2–500 eV/atom.

3. Results and discussion

3.1. Source of reflection and sputtering

The total sputtering yield of cluster impacting can be divided into two contributions, i.e. sputtered atoms from target and reflected atoms from cluster, $Y_{\text{total}} = Y + R$. Fig. 1 investigates the original locations of sputtered and reflected atoms in order to study the source of sputtering and reflections. The slash shadow part is the profile of final state of cluster–target interactions, where a significant crater forms. The points stand for the original location of sputtered and reflected atoms. There is no significant place tendency of reflection in cluster, which means cluster atoms are uniform randomly reflected. We also used broken and half spherical clusters to perform the same simulation and still no significant place tendency is found. So we reasonably conclude that the distribution of reflected atoms is independent on the shape of cluster.

But for target material, most of the sputtered atoms concentrate in the conical region just under the landing point of cluster, which is the region 1 in Fig. 1. The dimension of region 1 is determined by the impacting energy of clusters. Region 2 is the space between sputtering region and crater surface. The atoms in this place are not sputtered out of target but to form interstitial atoms and penetrate into deeper part of the material. The place labeled region 3 is not significantly influenced by cluster impacting. It is obvious that the volume of region 1 is the key factor which determines the sputtering yield Y .

3.2. Reflection and sputtering yield

Fig. 2 shows the reflection rate as a function of normalized incident energy $\epsilon = E/(NU)$. E is the total kinetic energy of cluster, U is the cohesive energy of target material, $U = 8.9$ eV for tungsten. N is the number of atoms in cluster, in Fig. 2, $N = 1036$. The reflection

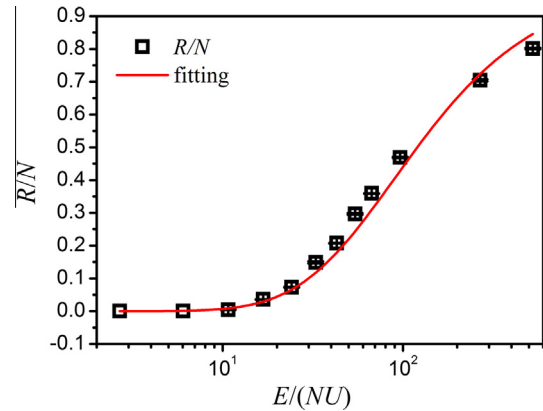


Fig. 2. Reflecting rate R/N as a function of impacting energy.

yield R is normalized by N . We find that when $\epsilon < 6$, the number of reflected atom R/N is zero. When $\epsilon > 6$, $R > 0$ but the increasing speed of R/N is slow. In such case, most of the cluster atoms are deposited on the target surface. When $\epsilon > 16$, more cluster atoms are sputtered so the increasing speed grows until $\epsilon \sim 250$. When $\epsilon > 250$, the increasing speed become slow again. This is because the reflection rate R/N cannot be over 1. The solid line in Fig. 2 is the fitting line using the following equation [30]:

$$\frac{R}{N} = \frac{\epsilon^f}{(\epsilon_c + \epsilon)^f} \quad (1)$$

where ϵ_c and f are fitting parameters, the values of them are 18 and 4.5, respectively. When $\epsilon \rightarrow 0$, $\frac{R}{N} \rightarrow 0$ and $\epsilon \rightarrow \infty$, $\frac{R}{N} \rightarrow 1$.

Anders and Urbassek simulated the reflection rate R/N of self-bombardment of Cu material [30]. The fitting parameters of Cu_{1000} is $\epsilon_c = 33$ and $f = 2.76$. The cohesive energy of copper U is selected 3.54 eV. R/N becomes quite close when $E/(NU) > 17$. But when impacting energy is less than this value, R/N of Cu cluster is greater than that of W. For example, when $E/(NU) = 6$, $R(\text{Cu})/N = 0.02$ while $R(\text{W})/N = 0$. This may be lead by different cohesive energy of cluster. The cohesive energy of Cu is 3.54 eV and 8.9 eV for W. In low energy case, Cu clusters are more easier to be reflected because Cu cluster is easier to be broken into atoms. The reflection rate of Ar_{1000} cluster in the same paper is greater than that of Cu, which supports the idea. The cohesive energy of Ar cluster is 0.082 eV.

Fig. 3 shows the comparison of sputtering yield and the number of atoms in sputtering region as a function of normalized incident

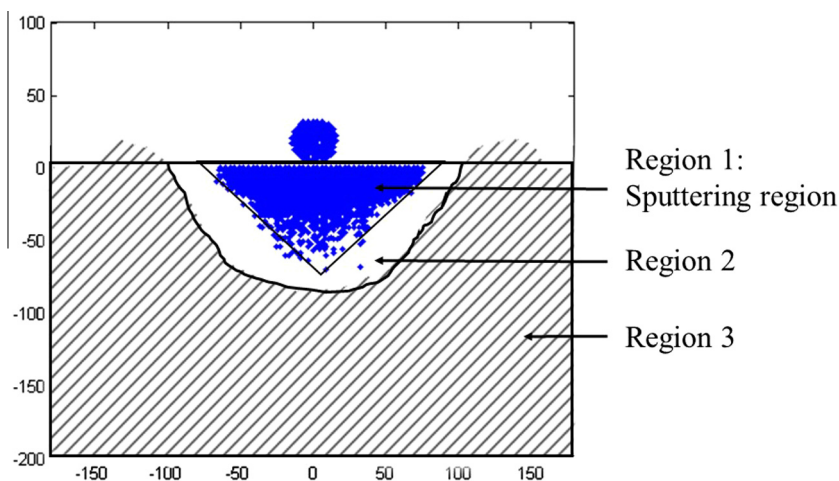


Fig. 1. Original location of sputtered atoms.

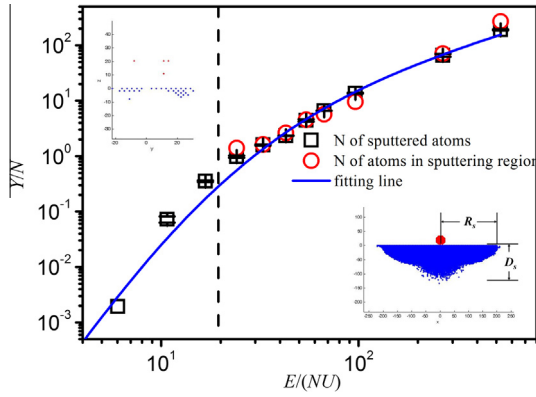


Fig. 3. Sputtering yield Y as a function of impacting energy.

energy ϵ . The solid line in Fig. 3 is the fitting curve using the following formula [30]:

$$Y = \frac{\alpha \epsilon^{1+b}}{(\epsilon_c + \epsilon)^b} \quad (2)$$

where α , b and ϵ_c are fitting parameters. ϵ_c is a threshold energy, when $\epsilon \gg \epsilon_c$, $Y \approx \alpha(\epsilon - b\epsilon_c)$ is a linear function of energy ϵ . When $\epsilon \ll \epsilon_c$, $Y \approx \alpha\epsilon_c \epsilon^{1+b}$. The parameters of the fitting line are $\alpha = 363$, $\epsilon_c = 20$ and $b = 45$.

The circles in Fig. 3 present the number of atoms in sputtering region Y' divided by N . In order to avoid losing generalization, we define $Y' = \rho_w \eta_c \eta_s V$. $V = \frac{1}{3} \pi R_s^2 D_s$ is the volume of conical, R_s and D_s is the radius and depth of conical, respectively, which is defined as the bottom-right subfigure in Fig. 2. ρ_w is the atom density of target. Because the sputtering region is not a perfect conical shape, we use η_c to describe the deviation of sputtering region from conical. The parameter η_s is the ratio of sputtered atoms to the total number of atoms in the conical. We set $\eta_c \sim 1$ and $\eta_s \sim 1$ in present study. For tungsten $\rho_w = 0.063 \text{ \AA}^{-3}$.

According to the original location of sputtered atoms, the sputtering process is different for low and high energy cluster impacting. In the low energy case, the sputtered atoms are discrete, as the top-left subfigure in Fig. 3, the counterpart impacting energy $E/(NU)$ is 2.68. The mechanism of sputtering process may be the shacking caused by collision of cluster. The sputter atoms are the ones obtaining enough kinetic energy from collision to escape from target surface. This mechanism is similar with the sputtering case of single ion impacting. No significant sputtering region forms in low energy impacting. So in such case, the sputtered atoms locates on the very surface of target, because the energy required to move an atom out of surface is less than that in the solid.

Energetic clusters, however, can destroy a large range on target surface. A conical continuous sputtering region is produced by impacting cluster. The vertical dash line in Fig. 3 divides the two cases. The left part of this line is discrete sputtering meanwhile the continuous region in the right, the corresponding energy scope is $0 \leq E/(NU) \leq 20$ and $E/(NU) \geq 20$, respectively. It can be seen that in the continuous region, the sputtering yield is consistent with the number of atoms in sputtering conical. Most of sputtered atoms is from the conical. It implies that we can investigate the depth D_s and radius R_s of sputtering region as a function of impacting energy.

Because the sputtering yield Y linearly depends on impacting energy ϵ , we fit the depth D_s and radius R_s of sputtering conical by power function $D_s = a_d + b_d \epsilon^{c_d}$ and $R_s = a_r + b_r \epsilon^{c_r}$ and we confirm the condition $2c_r + c_d = 1$. This condition can ensure that the sputtering yield Y is basically proportion to ϵ .

The fitting functions of conical depth and radius are

$$D_s = -24 + 11\epsilon^{0.4} \quad (3)$$

$$R_s = -79 + 38\epsilon^{0.3} \quad (4)$$

respectively, as shown in Fig. 4.

The square and circle points present R_s and D_s , respectively. The solid and broken lines are the fitting curve for R_s and D_s , respectively. The curves fit well with the simulation results except the conical radius R_s at low incident energy. Actually, the sputtering region is not a perfect conical shape and the bottom of it is not a round circle, either. As the increasing of impacting energy, the sputtering region become more and more close to conical shape. But in low energy cases, the sputtering region is not regular. One of the possible reasons of irregular shape is anisotropism of target lattice, and the other one may be the fluctuations of sputtering probabilities. When the impacting energy is large enough, both the reasons become ignorable, so the sputtering region tends to conical shape.

3.3. Size dependence of sputtering and reflection

The size dependence of reflection rate is shown in Fig. 5. The cluster ranges from 66 to 2647 atoms and the impacting energy is 850 eV/atom. The square points stand for the reflection rate. It can be seen that the reflection rate linearly dependent on cluster size and the slope is about 0.00012. Of course, when the size of cluster become larger, the R/N will not be linear on N because the maximum value of R/N is unity. But in the range $N < 2647$, the size dependence function is linear.

The sputtering yield is shown in Fig. 6. We can see that the sputtering yield of W clusters also linearly dependent on cluster size N and the slope is 0.006.

3.4. Temperature dependence of sputtering and reflection

We also investigate the temperature dependence of sputtering and reflection, as shown in Table 1. The meaning of columns are sequentially kinetic energy of cluster ϵ , temperature of target surface T , number of reflected and sputtered atoms.

The reflected and sputtered yield is zero when $\epsilon = 1$ and $T < 650 \text{ K}$ but at $T = 650 \text{ K}$, $R = 9$, $Y = 46$. This means when temperature of target surface is greater enough, the sputtering threshold energy is deduced, although the reflection rate and sputtering yield is small. The reason is that the thermo motion makes the atoms easier to escape from surface.

On the other hand, when the impact energy ϵ is greater than threshold value, the growth of T promotes the sputtering yield Y . However, the promotion effect is not significant for the reflection yield. The reason may be that R is not large, so the number is more

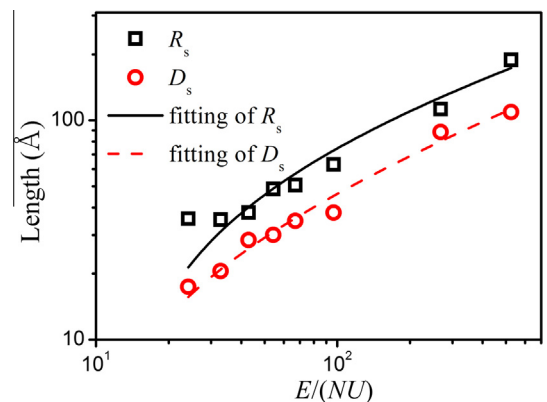


Fig. 4. Depth D_s and radius R_s of conicals as a function of impacting energy.

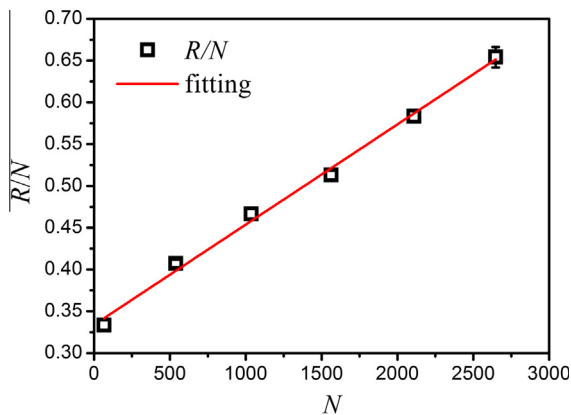


Fig. 5. Reflection rate R/N as a function of cluster size N .

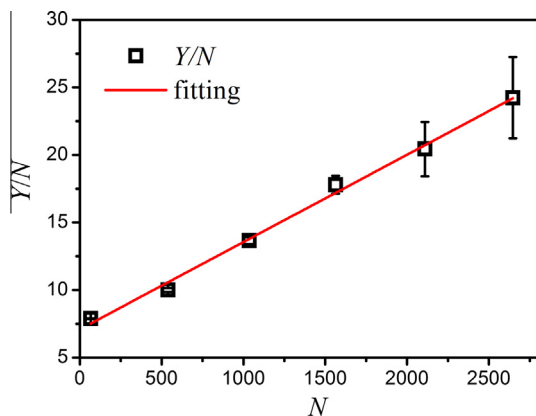


Fig. 6. Sputtering yield Y/N as a function of cluster size N .

Table 1
Y and R as a function of ϵ and T.

ϵ	T (K)	R	Y
1	0	0	0
1	300	0	0
1	650	9	46
10	0	82	2.5×10^3
10	300	86	3.09×10^3
10	650	107	5.92×10^3
100	0	4.18×10^2	7.96×10^4
100	300	4.05×10^2	9.19×10^4
100	650	4.17×10^2	1.09×10^5

likely to be influenced by fluctuation of probabilities. But the sputtering yield Y is more stable in statistics.

4. Conclusion

In present research, we investigate the sputtering yield and reflection rate of self-bombardment of tungsten material. According to the molecular dynamics simulation, the following conclusions are obtained:

1. The atoms in cluster are randomly reflected, and no specific location tendency in cluster is found. The reflected rate of W material is close to that of Cu in high impacting energy. But in low energy case, the reflected rate of W is less than Cu which may be led by the higher cohesive energy. But the sputtered atoms basically locate in the sputtering region. Sputtering region is a conical region just under the landing point.

2. According to the impacting energy, two different cluster sputtering mechanism are demonstrated. In the low impacting energy case, discrete atoms are sputtered. The sputtered atoms basically locate on the very surface of target, where the escaping energy is lower comparing with the inner part of target. But when the impacting energy is large enough, the sputtering region is continuous. The sputtering region is a conical just under the landing point. The number of atoms in this region are quite close to the sputtering yield which means almost all of the atoms in this region are sputtered atoms. The depth and radius of conical are related to the cluster energy. The depth $\propto \epsilon^{0.4}$ and radius $\propto \epsilon^{0.3}$ where ϵ is the normalized impacting energy.
3. The influence of cluster size on reflection and sputtering yield is also investigated in present research. In the cluster size ranging from 66 to 2647, both reflection rate and sputtering yield linearly dependent on cluster size.
4. The increasing of target surface temperature can increase the sputtering yield by clusters. Even when the impacting energy is less than sputtering threshold, high temperature target may produce sputtered atoms. On the other hand, the temperature of target influence the reflection rate weakly.

Acknowledgements

This work was supported by National Magnetic Confinement Fusion Science Program under Contracts Nos. 2013GB105001, 2013GB105002 and 2015GB109001, National Natural Science Foundation of China (NSFC) with Grant Nos. 11205198, 11305213 and 11405201, as well as Technological Development Grant of Hefei Science Center of CAS under contract No. 2014TDG-HSC003. The authors gratefully acknowledge the operation team of HIRFL for their help.

References

- [1] N. Ning, S.M. Rinaldi, H. Vach, An atomic-scale study of hydrogenated silicon cluster deposition on a crystalline silicon surface, *Thin Solid Films* 517 (23) (2009) 6234–6238.
- [2] Z. Ebrahimejad, S.F. Masoudi, R.S. Dariani, S.S. Jahromi, Thin film growth by deposition of randomly shaped clusters, *J. Chem. Phys.* 137 (15) (2012) 154703.
- [3] V.N. Popok, I. Barke, E.E.B. Campbell, K.H. Meiwes-Broer, Cluster-surface interaction: from soft landing to implantation, *Surf. Sci. Rep.* 66 (10) (2011) 347–377.
- [4] V.N. Popok, Cluster ion implantation in graphite and diamond: radiation damage and stopping of cluster constituents, *Rev. Adv. Mater. Sci.* 38 (1) (2014) 7–16.
- [5] Z. Insepov, I. Yamada, M. Sosnowski, Surface smoothing with energetic cluster beams, *J. Vac. Sci. Technol., A* 15 (3) (1997) 981–984.
- [6] K. Mochiji, N. Se, N. Inui, K. Moritani, Mass spectrometric analysis of the dissociation of argon cluster ions in collision with several kinds of metal, *Rapid Commun. Mass Spectrom.* 28 (19) (2014) 2141–2146.
- [7] E.J. Teo, N. Toyoda, C.Y. Yang, A.A. Bettiol, J.H. Teng, Nanoscale smoothing of plasmonic films and structures using gas cluster ion beam irradiation, *Appl. Phys. A* 117 (2) (2014) 719–723.
- [8] I. Yamada, J. Matsuo, Z. Insepov, M. Akizuki, Surface modifications by gas cluster ion beams, *Nucl. Instr. Meth. Phys. Res. Sect. B* 106 (1–4) (1995) 165–169.
- [9] G.H. Takaoka, H. Ryuto, M. Takeuchi, H. Kobayashi, Irradiation effect of gas-hydrate cluster ions on solid surfaces, *Nucl. Instr. Meth. Phys. Res. Sect. B* 326 (2014) 190–194.
- [10] Z. Insepov, A. Hassanein, D. Swenson, M. Terasawa, Computer simulation of surface modification with ion beams, *Nucl. Instr. Meth. Phys. Res. Sect. B* 241 (1–4) (2005) 496–500.
- [11] H. Haberland, Z. Insepov, M. Moseler, Molecular-dynamics simulation of thin-film growth by energetic cluster-impact, *Phys. Rev. B* 51 (16) (1995) 11061–11067.
- [12] M. Schwartzkopf, A. Buffet, V. Korstgens, E. Metwalli, K. Schlage, G. Benecke, J. Perlich, M. Rawolle, A. Rothkirch, B. Heidmann, G. Herzog, P. Muller-Buschbaum, R. Rohlsberger, R. Gehrke, N. Stribeck, S.V. Roth, From atoms to layers: in situ gold cluster growth kinetics during sputter deposition, *Nanoscale* 5 (11) (2013) 5053–5062.
- [13] C. Szakal, J. Kozole, M. Russo, B. Garrison, N. Winograd, Surface sensitivity in cluster-ion-induced sputtering, *Phys. Rev. Lett.* 96 (2006) 216104.

- [14] A. Wucher, Molecular secondary ion formation under cluster bombardment: a fundamental review, *Appl. Surf. Sci.* 252 (19) (2006) 6482–6489.
- [15] B.T. Draine, Interstellar dust grains, *Annu. Rev. Astron. Astr.* 41 (2003) 241–289.
- [16] V.N. Popok, Energetic cluster ion beams: modification of surfaces and shallow layers, *Mat. Sci. Eng. R* 72 (7–8) (2011) 137–157.
- [17] S.X. Zhang, H.F. Gong, X.Z. Chen, G.P. Li, Z.G. Wang, Low energy Cu clusters slow deposition on a Fe (001) surface investigated by molecular dynamics simulation, *Appl. Surf. Sci.* 314 (2014) 433–442.
- [18] A. Majumdar, M. Ganeva, D. Kopp, D. Datta, P. Mishra, S. Bhattacharaya, D. Ghose, R. Hippler, Surface morphology and composition of films grown by size-selected Cu nanoclusters, *Vacuum* 83 (4) (2008) 719–723.
- [19] V.N. Popok, Energetic cluster ion beams: modification of surfaces and shallow layers, *Mater. Sci. Eng. R* 72 (7–8) (2011) 137–157.
- [20] H.S. Araghi, Z. Zabihi, Molecular dynamics simulation of microscopic processes in Cu nanocluster impact onto Cu (001) substrate, *Nucl. Instr. Meth. Phys. Res. Sect. B* 298 (2013) 13–18.
- [21] T. Aoki, Molecular dynamics simulations of cluster impacts on solid targets: implantation, surface modification, and sputtering, *J. Comput. Electron.* 13 (1) (2014) 108–121.
- [22] C. Anders, H.M. Urbassek, R.E. Johnson, Linearity and additivity in cluster-induced sputtering: a molecular-dynamics study of van der Waals bonded systems, *Phys. Rev. B* 70 (15) (2004) 155404.
- [23] A. Wucher, Sputtering: experiment, ion beam science: solved and unsolved problems, *Pts 1 and 2* 52 (2006) 405–432, URL Go to ISI://WOS:000244649900016.
- [24] R.P. Webb, What do we want from computer simulation of sputtering using clusters?, *Appl. Surf. Sci.* 255 (4) (2008) 1223–1228.
- [25] C. Mucksch, C. Anders, H. Gnaser, H.M. Urbassek, Dynamics of l-phenylalanine sputtering by argon cluster bombardment, *J. Phys. Chem. C* 118 (15) (2014) 7962–7970.
- [26] Z. Insepov, I. Yamada, Molecular-dynamics simulation of cluster ion-bombardment of solid-surfaces, *Nucl. Instr. Meth. Phys. Res. Sect. B* 99 (1–4) (1995) 248–252.
- [27] R.P. Webb, The computer simulation of energetic cluster–solid interactions, *Radiat. Eff. Defects Solids* 162 (7–8) (2007) 567–572.
- [28] H. Kitani, N. Toyoda, J. Matsuo, I. Yamada, Incident angle dependence of the sputtering effect of Ar–cluster–ion bombardment, *Nucl. Instr. Meth. Phys. Res. Sect. B* 121 (14) (1997) 489–492.
- [29] C. Anders, H.M. Urbassek, Effect of binding energy and mass in cluster-induced sputtering of van-der-Waals bonded systems, *Nucl. Instr. Meth. Phys. Res. Sect. B* 228 (14) (2005) 84–91.
- [30] C. Anders, H.M. Urbassek, Sputtering and reflection under cluster bombardment of solids, *Nucl. Instr. Meth. Phys. Res. Sect. B* 315 (2013) 304–307.
- [31] <http://lammps.sandia.gov/>.
- [32] M.W. Finnis, J.E. Sinclair, A simple empirical n-body potential for transition-metals, *Philos. Mag. A* 50 (1) (1984) 45–55.
- [33] J.F. Ziegler, J.P. Biersack, U. Littmark, *Stopping and Ranges of Ions in Matter*, vol. 1, Pergamon Press, 1985.